Biochimica et Biophysica Acta, 765 (1984) 97–105
Elsevier

BBA 41473

STRUCTURAL CHANGES ACCOMPANYING THE IRREVERSIBLE OXIDATION OF THE CHROMATOPHORE MEMBRANE FROM *RHODOSPIRILLUM RUBRUM* G9

R. GHOSH [a], R. BACHOFEN [b] and H. HAUSER [a]

[a] *Laboratorium für Biochemie, ETH-Zürich, CH-8092, and* [b] *Institut für Pflanzenbiologie, Universität Zürich, CH-8008 Zürich (Switzerland)*

(Received December 1st, 1983)

Key words: Chromatophore membrane; Photooxidation; (R. rubrum)

The structure of the chromatophore membrane of the carotenoid-free mutant *Rhodospirillum rubrum* G9 and the effect of irreversible photooxidation upon this structure have been investigated using several physical techniques. Native chromatophore membranes undergo endothermic transitions in two temperature regions; at temperatures of about 0°C a broad reversible transition and between approx. 50 and 90°C several endothermic transitions are observed which are irreversible. The first transition can be assigned to the gel-to-liquid crystal transition of the lipid bilayer present in chromatophores; the irreversible one is attributed to changes mainly in the quarternary and possibily tertiary structure of membrane proteins. CD measurements showed that heating of chromatophores up to 70°C has no effect upon the protein secondary structure. Photooxidation has little effect on the structure and dynamics of the lipid bilayer in the chromatophore membrane. The order (or average conformation) of both the lipid polar groups and the hydrocarbon chains is hardly changed. However, the lipid phase transition is dramatically broadened and the protein-associated endothermic transitions are greatly reduced. This indicates that the major effect of photooxidation is upon lipid-protein and protein-protein interactions. Electron microscopy studies support this interpretation. It can be shown that the dense and regular packing of protein particles observed in the chromatophore membrane is lost as an effect of photooxidation. Instead, randomly distributed particles of varying size and shape are seen. These results are interpreted to mean that pigment-protein interactions are responsible for maintaining the native long-range order in the chromatophore membrane of *R. rubrum* G9. Destruction of the pigments by photooxidation leads to irreversible protein dissociation which in turn is followed probably by random protein reaggregation.

Introduction

In recent years various components of the photosynthetic electron transport chain in the chromatophores of purple, non-sulfur bacteria such as *Rhodospirillum rubrum* and *Rhodopseudomonas sphaeroides* have been isolated and some of their properties have been studied in isolated systems (e.g. Refs. 1–3). Biophysical studies on the intact chromatophore membrane have been performed in order to measure optical and other properties of single membrane components in situ, e.g., of the photoreaction center. As the absorbance of the bacteriochlorophyll of the light-harvesting complex(es) dominate(s) the long wavelength region, its contribution has to be eliminated when studying the properties of reaction centers. This was accomplished by specifically bleaching the pigment of the light-harvesting complex(es) using weak tungsten illumination in the presence of an oxidant. Under these conditions the activity and the bacteriochlorophyll of reaction centers re-

mained intact [4–6]. In this communication we show that the process of photooxidation causes a profound change in the native structure of the chromatophore membrane isolated from the carotenoid-free mutant, *R. rubrum* G9. This indicates that results obtained from irreversibly photooxidized membranes must be interpreted with great care.

Materials and Methods

Growth of the organism and preparation of the chromatophores. Cultures of about 1 l of the carotenoid-free mutant *R. rubrum* G9 were grown at low light intensity as described previously and chromatophores prepared by published procedures [7]. Chromatophore preparations were used immediately after preparation or alternatively stored in pellet form at −22°C and resuspended in buffer prior to use. Similar results were obtained with both preparations. Unless otherwise stated the buffer used was 10 mM Tris-HCl (pH 8.0), 5.0 mM EDTA. All operations were performed in a darkened room. Protein concentrations were determined using the modified Lowry assay as described by Peterson [8]. Chromatophore lipids were analysed by thin-layer chromatography (TLC) using $CHCl_3/CH_3OH/H_2O$ (85 : 30 : 3, v/v) as the solvent. Spots were detected by iodine vapour followed by detection with a molybdate and a ninhydrin spray.

Irreversible photooxidation of the chromatophores. Photooxidation was carried out according to Beugeling [4] by suspending chromatophores in the Tris buffer containing 0.1 M $K_3Fe(CN)_6$ to give an absorption at 875 nm of approx. 0.8. This suspension was illuminated at room temperature using a 60 W tungsten lamp at a distance of 1 m from the sample (light intensity 0.14 mW/cm^2) over a period of up to 3 days. The spectral changes were followed continuously during this time. Absorption spectra were recorded on a Uvikon 810 or a Zeiss PMQ II spectrophotometer equipped with a PbS detector.

Preparation of the samples for electron microscopy. Chromatophores were dispersed in the above buffer and dialyzed against 2 mM glutaraldehyde at 4°C overnight. The chromatophores were transfered into the buffer containing 25% glycerol either by centrifugation or by dialysis. Finally, the samples were centrifuged at 100 000 × *g* for 45 min to yield a hard pellet. Freeze-fracture electron microscopy was performed using the propane jet method [9].

Circular dichroism. Circular dichroism (CD) spectra were taken with a Cary 61 spectropolarimeter using thermostatically controlled 0.1 mm path-length cells at 28°C. Spectra were measured at the slowest possible speed and the baseline was run after each spectrum. With this instrument it was not possible to measure the bacteriochlorophyll exciton which occurs between 800 and 900 nm [10].

Differential scanning calorimetry. Differential scanning calorimetry (DSC) was performed using a Perkin/Elmer model DSC 2 instrument. Pelleted chromatophores were scraped into stainless steel pans which were hermetically sealed by pressure and immediately transferred to the DSC instrument. Before the measurements, the cells were cooled quickly to 255 K and then heated to the prescribed temperature at a rate of 2.5 K/min. Below approx. 255 K, the large exothermic peak due to the freezing of water made the observation of thermotropic events in this region impossible.

^{31}P-nuclear magnetic resonance. ^{31}P-NMR spectra were obtained using a Bruker CXP 300 spectrometer operating at 121.47 Mz in the Fourier transform mode. The spectral width was 31.25 kHz and a line-broadening of 100 Hz was used for all spectra. Spectra were accumulated using the Hahn spin echo sequence, $(90(+X) - \tau - 180(+X) - \tau - AQ - PD)_n$ with a 90° pulse of 3 μs, a refocussing time (τ) of 90 μs, an aquisition time (AQ) of 150 ms, and a pulse delay time (PD) of 8–10 s. The tuning of the decoupler was checked frequently using a pellet of dioleoyl phosphatidylcholine dispersed in the same buffer as a standard. All samples were prepared in pellet form in 10 mm glass sample tubes immediately prior to use. T_1-relaxation measurements were performed using a $(180(+X) - \tau - 90(+X) - AQ - PD)_n$ pulse sequence, where τ was varied from 1 ms to 9 s. The relaxation times were found to be independent of chemical shift; hence T_1 values were derived from the most intense peak of the powder spectrum (corresponding to $\sigma_\perp$) using a linear least-squares routine.

Electron spin resonance. The fatty acid spin label, 2-(3-carboxypropyl)-4,4-dimethyl-2-tridecyl-3-oxazolidinyloxyl (5-doxylstearic acid) was incorporated into the chromatophore membrane and ESR spectra were recorded at 9.16 GHz using a Varian X-band spectrometer as described previously [11]. The order parameter S_{33} [12] was derived as shown before [11]. Spectra were measured using the following temperature sequence: measurements were started at 30°C and the sample was subsequently cooled in 2°-steps to −30°C. The sample was then warmed slowly to 30°C and then heated in 2°-steps to 60°C. Measurements to 80°C were made in 5°-steps. Chromatophores were quite stable over several days when stored at 4° and the variation of the hyperfine splitting with temperature was completely reversible.

Results

Photooxidation of the antennae pigments

Oxidized chromatophores were produced by different treatments: first, according to Beugeling [4], this caused a slow decrease of the peak at 875 nm with a concomitant wavelength shift of about 25 nm (Fig. 1). A similar effect has been noted by Rafferty et al. [13] for chromatophores of *Rps. sphaeroides* and is thought to indicate the loss of paired bacteriochlorophyll molecules being able to form an exciton [13]. As the peak at 875 nm decreased, two peaks at shorter wavelength developed and in fully oxidized samples absorption maxima at approx. 690 and 810 nm were observed.

In contrast, the method of oxidation of Mar et al. [6], where the Tris buffer is replaced by distilled water, is more drastic: even after a few minutes the peak at 875 nm disappeared and was replaced by two peaks at 720 nm and 830 nm. The final product after approx. 12 h was quite similar to that produced when the samples were illuminated in Tris buffer [4]. It is important to note that very similar spectral changes were also observed in the presence of 0.1 M $K_3(Fe(CN)_6)$ in buffer but in the dark.

In contrast to the above-mentioned methods of photooxidation, samples were mildly oxidized in the dark: to the sample (4 mg protein/ml) dispersed in Tris buffer at 4°C $K_3Fe(CN)_6$ was added to a final concentration of approx. 1 mM. The resulting samples were identical in behaviour to photooxidized preparations as evident from electron microscopy and NMR spectroscopy. Their near infrared spectra were very similar to that of a sample photooxidized for 72 h according to Beugeling [4] (see Fig. 1).

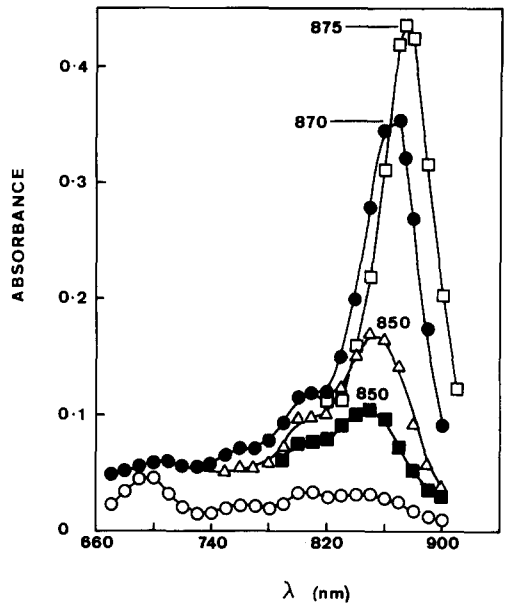

Fig. 1. Near infrared spectra of chromatophore membranes dispersed in Tris buffer (10 mM Tris-HCl (pH 8.0)/5 mM EDTA) after photooxidation in the presence of 0.1 $MK_3Fe(CN)_6$ at room temperature for different periods of time according to Beugeling [4]: control (□); 10 min (●); 12 h (△); 24 h (■); 72 h (○).

Electron microscopy of native and photooxidized chromatophores

The effect of photooxidation upon the supramolecular structures of the chromatophore membrane was examined by electron microscopy using propane jet freezing with and without cryoprotectant. In both cases similar results were obtained. Electron micrographs of cryoprotected, freeze-fractured samples are shown in Fig. 2. Native chromatophore membranes from *R. rubrum* form vesicles, the fracture faces of which appear to be covered with densely and fairly regularly packed spherical particles of approx. 12 nm diameter (Fig. 2a). Similar structures have been observed previously [14]. Upon irreversible photooxidation the membranes assume a much altered appearance

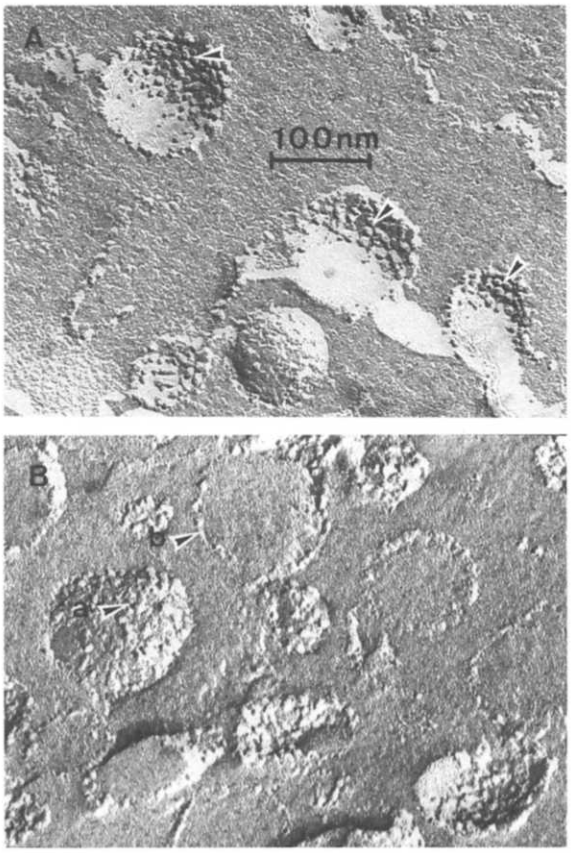

Fig. 2. Electron micrographs of freeze-fractured chromatophore membranes using 25% glycerol as a cryoprotectant: (A) native membranes, arrows indicate particular structures within the membrane that show dense and fairly regular packing; (B) membranes photooxidized according to Ref. 4. The arrows indicate (a) the lack of structure within the membrane; (b) a cross-section through a vesicle.

(Fig. 2b). The regular packing of the particles is lost and frequently particle aggregation to larger irregular structures can be observed (see arrow a, Fig. 2b). A further interesting feature of the electron micrographs is the observation of many cross-sections of vesicles that have apparently been cleaved perpendicular to the bilayer plane (see arrow b, Fig. 2b).

Circular dichroism studies of the chromatophore membrane

The effect of oxidation upon the secondary structure of the membrane proteins of the chromatophore membrane was determined by CD. CD spectra in the near ultraviolet region of native and oxidized chromatophores are shown in Fig. 3. These two spectra are very similar: they show minima at 222 and 208 nm and a cross-over point at 202 nm characteristic of a predominantly α-helical structure. This conclusion is consistent with results obtained using polarized infrared spectroscopy of intact chromatophore membranes [15]. Photooxidation did not produce any significant changes in the CD spectrum. Possible interference from light-scattering was checked by measuring chromatophores sonicated for approx. 5 min. The CD spectrum remained unchanged. Furthermore, there was no significant change in the CD spectra when chromatophore membranes were heated up to approx. 70°C. We conclude from this that heating native chromatophore membranes up to 70°C has no apparent effect on the secondary structure of integral membrane proteins.

Effect of photooxidation upon the lipids of the chromatophore membrane

Lipid compositon determined by TLC analysis. Illumination of chromatophore lipids and pigments extracted from native membranes caused rapid oxidative degradation of the lipids due to the

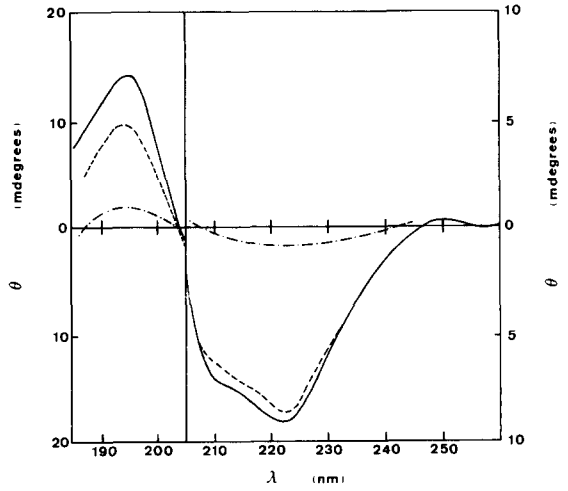

Fig. 3. Circular dichroic (CD) spectra of native (———) and photooxidized membranes (- - - - - -). For the region below approx. 205 nm a different y-axis is used left-hand panel). The intermittently dashed line (·—·—·) is the base-line.

production of bacteriochlorophyll radicals. This was readily observed as 'streaking' in the TLC analysis. In principle, lipid degradation might also occur in membranes that have been irreversibly oxidized. That this is not the case is demonstrated by TLC analysis of the lipid extract of oxidised chromatophores. The relative R_f values of the lipids extracted from oxidized membranes were identical to those from native membranes. Both extracts gave several and identical spots which were identified as phosphatidylethanolamine, phosphatidylglycerol, cardiolipin and a red pigment, probably rhodoquinone. We conclude, therefore, that the lipids are not photolytically degraded during photooxidation of the chromatophores.

Calorimetric studies. Fig. 4 shows heating curves obtained by DSC of native and photooxidized membranes. Native chromatophores showed two main transitions, a broad one between about −10°C and another transition region between about 50 and 90°C with peak temperatures of 54 and 60°C and a broad hump at approx. 80°C. The low-temperature transition was fully reversible: cooling scans showed an exothermic transition shifted by a few degrees towards lower temperatures (data not shown). A second heating curve (b (dashed line)) was recorded after heating native chromatophores to approx. 90°C and cooling them

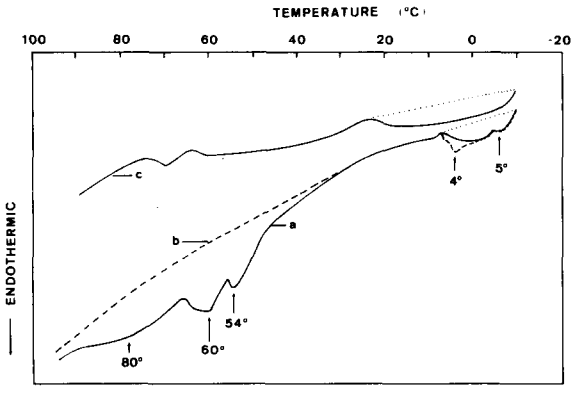

Fig. 4. Differential scanning calorimetry (DSC) of native (a, b) and photooxidized (c) chromatophore membranes. Only the heating scans are shown. (a) and (b) represent the first and second heating run of the same membrane sample, respectively. The dotted line (· · · · · ·) represents the extrapolated baseline for the lipid transition.

to about −15°C. The enthalpy of the low-temperature transition was increased slightly, whereas the high-temperature transition was completely abolished. Based on these observations, the low- and high-temperature transitions were assigned to lipids and proteins, respectively. The reversible lipid transition is probably a gel-to-liquid crystal phase transition of the phospholipid bilayer. It was, however, not possible to observe the complete transition due to the interference from the freezing of water, which in a membrane pellet occurred at approx. −15°C. For the phospholipid phase transition the (dotted) base-line was obtained by extrapolating the base-line from the high-temperature end of the scan. However, this extrapolated base-line is arbitrary and does not allow us to derive enthalpies from the peak areas. In contrast to native chromatophores, photooxidized membranes gave a much broader reversible lipid phase transition between about −10 and +25°C (curve c, Fig. 4). Furthermore, the high-temperature transitions were almost absent, or at least greatly reduced.

^{31}P NMR studies. In Fig. 5a and b the ^{31}P powder-type NMR spectra obtained from pellets of native and photooxidized chromatophores are compared. For both native and photooxidized membranes the ^{31}P NMR spectra are typical for non-oriented lipid bilayers with the phospholipid molecule as a whole and/or the phosphodiester group undergoing fast motion about an axis parallel to the bilayer normal. This rapid motion of the phosphate group leeds to a time-averaged, axially symmetric shielding tensor. The shielding anisotropy $\Delta\sigma = \sigma_{\parallel} - \sigma_{\perp}$ is −41 ppm for native chromatophore membranes in the liquid crystalline state at 10–20°C (Fig. 5a). This agrees within the experimental error with the shielding anisotropy measured in aqueous dispersions of phosphatidylethanolamine or phosphatidylglycerol above the gel-to-liquid crystal phase transition [17,18]. The chromatophore lipids consist of 65% phosphatidylethanolamine, 25% phosphatidylglycerol, 10% cardiolipin [7]; hence the ^{31}P NMR spectrum of chromatophores is expected to be a superposition essentially of the phosphatidylglycerol and phosphatidylethanolamine spectra. This is indeed born out by the ^{31}P NMR spectra shown in Fig. 5a. In the photooxidized state $\Delta\sigma = \sigma_{\parallel} - \sigma_{\perp}$ is only

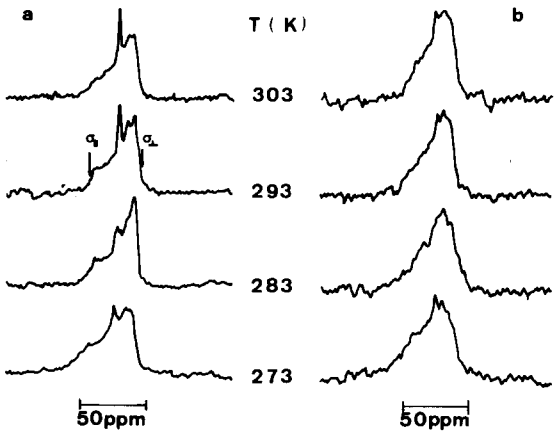

Fig. 5. ^{31}P NMR spectra of native (a) and photooxidized (b) membranes at different temperatures. Spectra were taken using the Hahn spin echo sequence and continuous broadband decoupling. Both sets of spectra were taken under identical conditions. Approx. 3–5 K scans were taken for each spectrum.

slightly larger by approx. 10% (Fig. 5b). However, the most noticeable difference is in the intrinsic linewidth which appears to be significantly larger for photooxidized membranes thus causing a 'smearing out' of the normal liquid crystalline powder pattern. This effect is particularly noticeable at the edge which corresponds to $\sigma_{\parallel}$ of the powder pattern (left-hand edge of the spectrum (Fig. 5b)) and which is smoothed out beyond detection. At 0°C where the chromatophore membrane is known to undergo the transition to the gel state (see Fig. 5a and b at 273 K) spectra of both native and photooxidized membranes become almost superimposable. Similar line broadening has also been noted by Tamm and Seelig [19] who applied ^{2}H NMR to artificial membranes assembled from palmitoyloleoyl phosphatidylcholine and cytochrome *c* oxidase. Line broadening was apparent at low lipid/protein ratios.

In all spectra shown (Fig. 5) a small isotropic peak was observed. Several lines of evidence suggest that this component is not due to the presence of inorganic phosphate in the bulk phase: (1) the chromatophores were prepared in the absence of phosphate; (2) the signal intensity was not affected by repeated washing of the chromatophores; (3) the isotropic peak did not decrease at temperatures below the freezing point of water; (4) the T_1 relaxation time of this component was almost identical to that of the bulk lipids, and (5) the apparent increase of the peak at higher temperatures was completely reversible. We suggest therefore that this component may arise from a small proportion (approx. 7%) of lipid present in small chromatophore vesicles (less than 80 nm) and/or present in a non-bilayer state [20–22].

We have measured the ^{31}P-T_1 relaxation time for the native and photooxidized membranes (data not shown). Native membranes in the liquid crystalline state gave a T_1 of approx. 1.2–1.4 s which is typical for aqueous phosphatidylcholine and phosphatidylethanolamine dispersions above the gel-to-liquid crystalline phase transition temperature [19–23]. In contrast, photooxidized membranes have a T_1 relaxation time that is shorter by a factor of 2–5. Short T_1 values were also obtained for samples which had been gently oxidized in the absence of $K_3Fe(CN)_6$ and which were measured in the presence of 5 mM EDTA; under these conditions the presence of paramagnetic impurities in the bulk water phase as a possible cause for decreasing the T_1 relaxation time can be ruled out.

ESR studies. The packing of the hydrocarbon chains in native and photooxidized chromatophore membranes was probed by incorporating 5-doxylstearic acid. Representative spectra are shown in Fig. 6. The ESR spectra of this spin probe in both types of membranes are consistent with the lipids being present as a bilayer and undergoing fast, anisotropic motion about the bilayer normal. The ESR results are consistent with the ^{31}P NMR data. Fig. 7a depicts the temperature dependence of the maximum hyperfine splitting $A_{\parallel}$ and the order parameter S_{33} for both native and photooxidized membranes. From the temperature dependence of both $A_{\parallel}$ and S_{33} (Fig. 7b) it is clear that the hydrocarbon chains in photooxidized membranes are similar if not more ordered than in native membranes. This trend continues up to approx. 55°C at which temperature the order becomes identical in both membranes. At the other end of the temperature range, the minimum hyperfine splitting becomes unobservable in both membranes at temperatures of 20°C or lower. Below approx. 20°C, the maximum hyperfine splitting $A_{\parallel}$ rises similarly in both membranes approaching the principal tensor component A_{zz} at approx. $-20°$ to $-30°$C (Fig. 7).

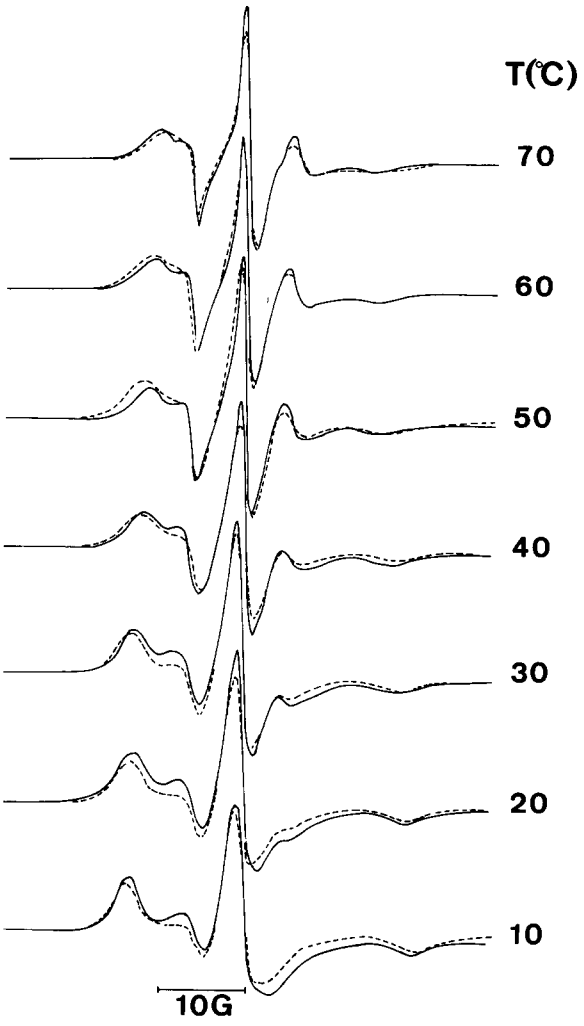

Fig. 6. Temperature dependence of the ESR spectra of 5-doxylstearic acid incorporated into native (———) and photo-oxidized (- - - - - -) chromatophore membranes dispersed in buffer. The phospholipid/spin label molar ratio was approx. 200:1.

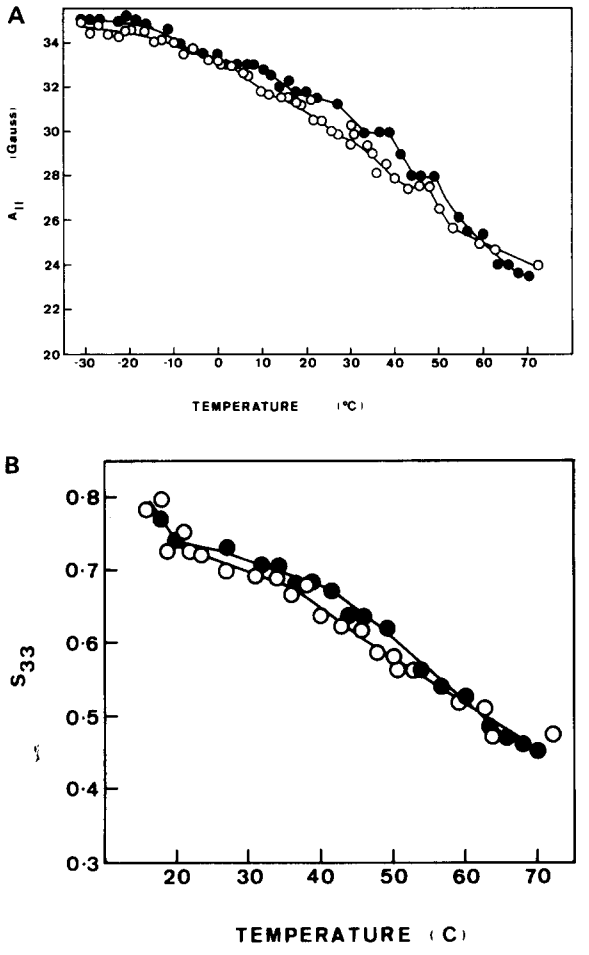

Fig. 7. (A) Temperature dependence of the maximum hyperfine splitting $A_{\parallel}$ for 5-doxylstearic acid incorporated into native (○) and photooxidized (●) chromatophore membranes. Both membranes were dispersed in 20 mM Tris/HCl (pH 8.0), 5 mM EDTA; photooxidized membranes were washed with the same buffer prior to measurement. (B) Temperature dependence of the order parameter (S_{33}) for the native (○) and photooxidized (●) membranes. Below approx. 10°C the minimum hyperfine splitting $A_{\perp}$ was no longer observable, and consequently order parameters could not be calculated at temperatures less than 10°C.

Discussion

In this study we have examined the effects of photooxidation of the antennae and reaction center pigments upon the molecular and supramolecular structure of the chromatophore membrane from *R. rubrum* G9. The primary event that occurs during irreversible photooxidation is either the degradation of the bacteriochlorophyll, probably to bound bacteriopheophytin a or a conformational change of the bacteriochlorophyll carrying proteins. Photooxidation has been used by several investigators to simplify spectral analysis of the intact membrane thus facilitating studies of component proteins in situ [4–6,24]. This paper shows that in the carotenoid-free mutant G9 photooxidation produced spectral changes which are indicative of profound structural alterations. Control experi-

ments with chromatophores of the wild type S1 demonstrate that similar but less pronounced spectral changes occur.

Freeze-fracture electron microscopy shows that photooxidative events gradually destroy the dense and regular packing of the 12 nm particles present in native membranes. The CD study clearly indicates that photooxidation or heating up to approx. 70°C of the chromatophore membrane has no effect on the protein secondary structure: the α-helical content remains unchanged. Considering the CD evidence, we attribute the irreversible, high temperature protein-associated transition observed with DSC to changes mainly in the quarternary protein structure and possibly in the tertiary structure. This probably involves the disruption of protein-protein interactions which leads to the dissociation of protein aggregates. In photooxidized membranes, these protein-associated transitions are reduced almost to zero indicating that photooxidation has a similar effect as heating the native membranes to about 90°. This interpretation of photooxidation in terms of protein disaggregations is consistent with the structural changes observed by electron microscopy: photooxidation causes the segregation of the 12-nm particles which may consist of several and probably different protein components. This disruption of regularly spaced arrays (Fig. 2a) may also be accompanied by the dissociation of proteins contained in a single 12-nm particle. In a secondary reaction, the dissociated proteins probably aggregate randomly to form large protein aggregates as evidenced by electron microscopy (Fig. 2b). The proposed structural changes induced by photooxidation are summarized in the following scheme:

regularly packed protein particles → disaggregation of protein particles

↓

random reaggregation ← dissociation of protein aggregates

In photooxidized membranes the reversible lipid transition appears to be broadened dramatically compared to native membranes (Fig. 4). Similar effects have been noted for the dissociation of the bacteriorhodopsin lattice in reconstituted membranes [25] which have been attributed to increased lipid-protein interfacial contacts. An alternative explanation would be that upon photooxidation the component proteins aggregate nonspecifically to large clumps within the membrane, trapping phospholipid molecules between them. These trapped phospholipids may give rise to a much broadened phase transition due to their different environment. Besides electron microscopy the formation of large protein aggregates is demonstrated by a different behaviour in gradient centrifugation: native membranes partially solubilized in 2% sodium cholate at pH 8.0 were subjected to a discontinuous sucrose gradient centrifugation; the single homogeneous band at the 1.2 M/2 M sucrose interface represented the nonsolubilized membrane fraction, while the solubilized membrane fraction was isolated at the 0.6 M/1.2 M interface. Treatment of photooxidized membranes with 2% cholate, however, always produced 'clumps' of protein at the 1.2 M/2 M interface: a homogeneous band was never obtained, nor a solubilized fraction at the 0.6 M/1.2 M interface.

The magnetic resonance data suggest that the effect of photooxidation upon the order or the motionally averaged conformation of the phospholipid head-groups and upon the packing of the hydrocarbon chains is relatively small. The ^{31}P NMR data indicate that the chemical shielding anisotropy is slightly increased by about 10% and ESR shows that the order of the hydrocarbon chain packing is slightly increased in photooxidized membranes. Two points of the ^{31}P NMR data are noteworthy. First, a characteristic feature of photooxidized membranes is the increase in the intrinsic line-width of the component lines of the ^{31}P NMR spectra. Similarly, broadened ^{31}P NMR spectra have been observed with the intact purple membrane of *Halobacterium halobium* (R. Ghosh and N.A. Dencher, unpublished results) and *Halobacterium cutirubrum* [26], where the phospholipids are known to be trapped within a protein matrix. These spectra can be fitted quite well using a large intrinsic linewidth. It is conceivable that in photooxidized membranes, phospholipids trapped within large protein aggregates may give

rise to a similar effect. Secondly, for all of the photooxidized samples measured, the ^{31}P-T_1 relaxation time was dramatically shorter than for the native membrane. We suggest that this short relaxation time arises due to the exposure of a metal ion during disaggregation of the 12-nm particles. As these particles have been shown to contain reaction centres [27–29] a possible candidate would be the tightly bound iron atom thereof. A similar effect has been observed by Tamm and Seelig [19] during the denaturation of cytochrome oxidase and has been shown to be due to the exposure of haem *a*-bound metal iron.

Conclusions

In summary we have shown that the bacteriochlorophyll bound to the light-harvesting complexes and possibly to the reaction centers is essential for maintaining the structural integrity of the chromatophore membrane of *R. rubrum* G9. It should be emphasized that these effects can be observed with membranes that have been only mildly oxidized, e.g., a shift in the near infrared absorption maximum from 875 to 870 nm is often sufficient to produce a loss of the regular packing of proteins in native chromatophore membranes and also a short ^{31}P-T_1 relaxation time. The study presented here clearly shows that great caution should be excercised in interpreting physical data obtained from bleached chromatophores. However, we have examined mainly the structural changes in the more sensitive carotenoid-free membranes from *R. rubrum* G9, whereas previous studies [4–6,13] have employed the wild type strains. However, several control experiments using the wild type S1 indicate that the difference between the two strains is more of a quantitative than a qualitative nature. The decrease in the far-red absorption and the spectral shift to lower wavelength was similar in both strains; it was markedly slowed down upon oxidation. The reaction-center activity measured as the reversible photobleaching of the P-870 pigment decreased with time similarly in both strains.

Acknowledgements

We thank Dr. V. Wiemken for her assistance in growing and handling *R. rubrum* G9. We wish also to acknowledge support from the Swiss National Science Foundation (Grant 3.582.79).

References

1 Cogdell, R.J. (1982) in Electron transport and photophosphorylation (Barber, J., ed.), pp. 177–196, Elsevier, Amsterdam
2 Feher, G. and Okamura, M.Y. (1978) in The photosynthetic Bacteria (Clayton, R.K. and Sistrom, W.R., eds.), pp. 119–131, Plenum Press, New York
3 Clayton, R.K. (1978) in The photosynthetic Bacteria (Clayton, R.K. and Sistrom, W.R., eds.), pp. 387–396, Plenum Press, New York
4 Beugeling, L. (1968) Biochim. Biophys. Acta 153, 143–153
5 Vermeglio, A. and Clayton, R.K. (1976) Biochim. Biophys. Acta 449, 500–515
6 Mar, T., Picorel, R. and Gingras, G. (1981) Biochim. Biophys. Acta 637, 546–550
7 Snozzi, M. and Bachofen, R. (1979) Biochim. Biophys. Acta 546, 236–247
8 Peterson, G.L. (1977) Anal. Biochem. 83, 346–356
9 Müller, M., Meister, N. and Moor, H. (1980) Mikroskopie 36, 129–140
10 Sauer, K. and Austin, L.A. (1978) Biochemistry 17, 2011–2019
11 Hauser, H., Gains, N., Semenza, G. and Spiess, M. (1982) Biochemistry 21, 5621–5628
12 Seelig, J. (1976) in Spin labelling. Theory and Application (Berliner, L.J., ed.), pp. 373–409, Academic Press, New York
13 Rafferty, C.N., Bolt, J., Sauer, K. and Clayton, R.K. (1979) Proc. Natl. Acad. Sci. U.S.A. 76, 4429–4432
14 Meyer, R., Snozzi, M. and Bachofen, R. (1981) Arch. Microbiol. 130, 125–128
15 Nabedryk, E. and Breton, J. (1981) Biochim. Biophys. Acta 635, 515–524
16 Seelig, J. (1977) Biochim. Biophys. Acta 515, 105–140
17 Seelig, J., Gally, H.U. and Wohlgemuth, R. (1977) Biochim. Biophys. Acta 467, 109–119
18 Büldt, G. and Wohlgemuth, R. (1981) J. Memb. Biol. 58, 81–100
19 Tamm, L. and Seelig, J. (1983) Biochemistry 22, 1474–1483
20 Burnell, E., Van Alphen, L., Verkleij, A. and De Kruijff, B. (1980) Biochim. Biophys. Acta 597, 492–501
21 De Kruijff, B., Van den Besselaar, A.M.H.P., Cullis, P.R., Van den Bosch, H. and Van Deenen, L.L.M. (1978) Biochim. Biophys. Acta 514, 1–8
22 Cullis, P.R., De Kruijff, B., Hope, M.J., Nayar, R., Rietveld, A. and Verkleij, A.J. (1980) Biochim. Biophys. Acta 600, 625–635
23 Seelig, J., Tamm, L., Hymel, L. and Fleischer, S. (1981) Biochemistry 20, 3922–3933
25 Heyn, M.P., Blume, A., Rehorek, M. and Dencher, N.A. (1981) Biochemistry 20, 7109–7115
26 Ekiel, I., Marsh, D., Smallbone, B.W., Kataes, M. and Smith, I.C.P. (1981) Biochem. Biophys. Res. Commun. 100, 105–110
27 Reed, D.W., Raveed, D. and Reporter, M. (1970) Biochim. Biophys. Acta 387, 368–378
28 Oelze, J., Biedermann, M. and Drews, G. (1969) Biochim. Biophys. Acta 173, 436–447
29 Valkirs, G., Rosen, D., Tokuyasu, K.T. and Feher, G. (1976) Biophys. J. 16, 223a